Efficient Resource Scheduling and Optimization for Over-Loaded LEO-Terrestrial Networks

Yaxiong Yuan[1], Lei Lei[1,2], Thang X. Vu[1], Scott Fowler[3], Symeon Chatzinotas[1]

[1]Interdisciplinary Centre for Security, Reliability and Trust (SnT), University of Luxembourg, Luxembourg
[2]School of Information and Communications Engineering, Xi'an Jiaotong University, China
[3]Department of Science and Technology, Linköping University, Sweden
Emails: {yaxiong.yuan; lei.lei; thang.vu; symeon.chatzinotas}@uni.lu, scott.fowler@liu.se

ICC 2022 - IEEE International Conference on Communications | 978-1-5386-8347-7/22/$31.00 ©2022 IEEE | DOI: 10.1109/ICC45855.2022.9839277

***Abstract*—Towards the next generation networks, low earth orbit (LEO) satellites have been considered as a promising component for beyond 5G networks. In this paper, we study downlink LEO-5G communication systems in a practical scenario, where the integrated LEO-terrestrial system is over-loaded by serving a number of terminals with high-volume traffic requests. Our goal is to optimize resource scheduling such that the amount of undelivered data and the number of unserved terminals can be minimized. Due to the inherent hardness of the formulated quadratic integer programming problem, the optimal algorithm requires unaffordable complexity. To solve the problem, we propose a near-optimal algorithm based on alternating direction method of multipliers (ADMM-HEU), which saves computational time by taking advantage of the distributed ADMM structure, and a low-complexity heuristic algorithm (LC-HEU), which is based on estimation and greedy methods. The results demonstrate the near-optimality of ADMM-HEU and the computational efficiency of LC-HEU compared to the benchmarks.**

***Index Terms*—LEO satellites, resource scheduling, supply-demand matching, ADMM, heuristic algorithm.**

I. Introduction

The next generation networks are expected to provide not only ubiquitous coverage but also extremely high data rate services [1]. In practical operations, terrestrial base stations (BSs) can become over-loaded and congested. This common issue has been received considerable attention from the academia, industry, and standardization bodies, e.g., 3GPP Release 17 [2]. Although conventional heterogeneous networks are able to offload data to improve the network capacity and service coverage, they face several issues such as limited backhaul resources of small cells and degradation of users' experience [3].

To enable cost-efficient broadband internet data services, SpaceX and OneWeb launch thousands of LEO satellites to deploy a dense constellation to support seamless communication services particularly for remote areas [4]. However, the communication schemes and resource management algorithms designed for terrestrial networks can not be used in LEO-assisted systems due to the differences, for example, in network topology and channel modeling [5]. For the frequency bands, the terrestrial communication applies C-band, e.g., sub-6GHz in 5G applications. Whereas, LEO satellite communication can adopt higher frequency bands, i.e., Ka-band, to access wider bandwidths as the radio frequency congestion becomes a serious issue in the lower bands due to the satellites' increased usage [4]. In LEO-assisted systems, instead of the traditional small cell base stations (SBSs), a dedicated terrestrial-satellite terminal (TST), equipped with steerable antennas, relies on LEO-assisted backhaul transmission and acts as the access point to provide a great number of users with a more flexible access technique.

In the literature, the tailored communication schemes have been investigated to improve the networks' performance, e.g., resource utilization and network throughput, for LEO-terrestrial networks. In [6], the authors proposed a user scheduling scheme to maximize the network throughput and the number of accessed users by utilizing the LEO-based backhaul. In [7], considering transmission delay, a user association scheme was proposed to maximize the network throughput in hierarchical LEO systems. In [8], the authors developed a joint resource block and power allocation algorithm to maximize the total transmission rate for LEO systems, where both LEO can offload data from BSs. The authors of [9] formulated an optimization problem to select the beam-hopping pattern, on-board power, and bandwidth for LEO systems. The proposed algorithms in [6]–[9] focus on improving the system throughput. However, there are still two main issues in over-loaded LEO systems that need to be addressed. Firstly, since not all users can be served with limited resources, designing a scheme that can guarantee user fairness and maximize the number of served users is important. Secondly, the volume of data requested by ground devices (GDs) varies significantly depending on different types of services, where GD includes TST and mobile terminal (MT). To explore more flexible and efficient communication schemes, it is necessary to consider the metric of matching error, i.e., the gap between the supply and the demand [10].

In this work, we aim to utilize LEO satellites to enhance the performance of over-loaded downlink communication systems. In particular, formulate a quadratic integer programming (QIP) problem to minimize the gap between demand and supply, and the gap between the number of minimum requirement-satisfied GDs and the total GDs via scheduling time slots to transmitter-GD pairs. Due to the combinatorial nature of the formulated QIP problem, the computational time for the optimal algorithm increases exponentially with the dimension of the problem. Thus, we develop two heuristic algorithms, i.e., alternating direction method of multipliers-based heuristic algorithm (ADMM-HEU) and low-complexity

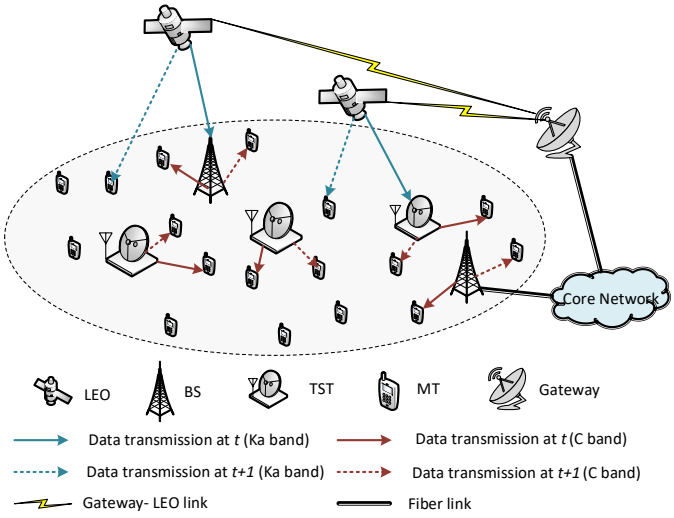

Figure 1. An illustrative system architecture

heuristic algorithm (LC-HEU), to reduce the computational time. In ADMM-HEU, the computational efficiency is improved by dividing the variables into multiple blocks which can be solved in parallel. In LC-HEU, the resource scheduling is accomplished based on estimation and greedy methods instead of consuming time to find the optimal solutions. Finally, we simulate different algorithms to compare their objective values and computational time. The results demonstrate the effectiveness of the proposed algorithms and their trade-offs between quality and efficiency.

The rest of the paper is organized as follows. We present the system model in Section II and formulate a resource scheduling problem in Section III. Two heuristic algorithms are proposed in Section IV. Numerical results are demonstrated in Section V. Finally, Section VI concludes the paper.

II. System Model

A. LEO-Terrestrial Network

As illustrated in Fig. 1, we consider a downlink over-loaded scenario, where the BSs with limited resources might not be able to serve all the users and deliver all the requested data demands within a required transmission or queuing delay. To relieve the burden of the terrestrial BSs, LEO satellites are introduced to offload traffic from BSs or provide backhauling services. The LEO employs a transparent payload and adopts Ka-band [4]. The terrestrial communication uses C-band [6]. Compared to conventional cellular BS, TST is a small-size terminal that acts as a flexible and cost-saving access point, which can either receive backhauling services from LEO over Ka-band or transmit data to MTs over C-band [6]. We consider two types of MTs that coexist in the system. The first type is the normal cellular terminals, e.g., cell phones, that can be served by BSs or TSTs, typically with large traffic demands. The other is the machine-type communication terminals, e.g., massive devices requesting lower data demands, which are equipped with a 3GPP terrestrial-non-terrestrial network (TN-NTN) compliant dual-mode that can be either served by LEO via Ka-band or by BS/TST through C-band [11]. The terrestrial BSs can request data from the core network through optical fiber links or from the LEO satellites through the BS-LEO link. We denote $\mathcal{K} = \{1, ..., k, ..., K\}$ as the union of GDs, including TSTs and MTs, and $\mathcal{N} = \{1, ..., n, ..., N\}$ as the union of transmitters. The set $\mathcal{N}$ can be further divided into two subsets $\mathcal{N}^{(1)}$ and $\mathcal{N}^{(2)}$, where $\mathcal{N}^{(1)}$ consists of the transmitters using Ka-band, i.e., LEO, while $\mathcal{N}^{(2)}$ contains the transmitters occupying C-band, i.e., BS or TST. We assume that the transmission tasks are delay-sensitive and should complete within T time slots. The time domain is divided by time slots, i.e., $\mathcal{T} = \{1, ..., t, ..., T\}$. In data transmission, a unicast mode is considered such that each transmitter n serves GD k in a one-to-one pattern, i.e., a transmitter-GD link (n, k). Within a time slot, multiple transmitter-GD links can be activated, forming a link group.

We remark that the network scale in Fig. 1 can be extended. Specifically, a GD in Fig. 1 can represent a cluster of densely-deployed devices. Due to the proximity, the channel states of the devices within a cluster can be assumed identical. When a cluster is scheduled, all the devices within the cluster will be scheduled by the TDMA (or FDMA) mode to avoid intra-cluster interference.

B. Link Groups

We denote $\mathcal{G} = \{1, ..., g, ..., G\}$ as the union of all possible transmitter-GD link groups and introduce binary parameters $\alpha_{k,n,g}$ to represent the activated links in a group, where $\alpha_{k,n,g} = 1$ means transmitter-GD link (n, k) is activated in group g, otherwise, 0. We can enumerate all the possible groups and calculate the parameters $\alpha_{k,n,g}$ based on the unicast constraints:

$$\sum\nolimits_{n\in\mathcal{N}} \alpha_{k,n,g} \le 1, \ \forall\ k \in \mathcal{K}, \ g \in \mathcal{G}, \tag{1}$$

$$\sum\nolimits_{k\in\mathcal{K}} \alpha_{k,n,g} \le 1, \ \forall\ n \in \mathcal{N}, \ g \in \mathcal{G}, \tag{2}$$

where (1) means that each GD k in group g receives data from at most one transmitter, and (2) represents each transmitter n in group g serves no more than one GD. Confined by (1) and (2), the SINR and delivered date to GD k in group g at time slot t can be expressed as:

$$\gamma_{k,g,t} = \frac{\sum_{n\in\mathcal{N}_1} h_{k,n,t}\alpha_{k,n,g}p_k}{\sum_{j\in\mathcal{K}\setminus k}\sum_{n\in\mathcal{N}_1} h_{j,n,t}\alpha_{j,n,g}p_k + \sigma^2} + \frac{\sum_{n\in\mathcal{N}_2} h_{k,n,t}\alpha_{k,n,g}p_k}{\sum_{j\in\mathcal{K}\setminus k}\sum_{n\in\mathcal{N}_2} h_{j,n,t}\alpha_{j,n,g}p_k + \sigma^2}. \tag{3}$$

and

$$R_{k,g,t} = \Phi B \log_2(1 + \gamma_{k,g,t}), \tag{4}$$

where p_k is the transmit power to GD k, $h_{k,n,t}$ is the channel state between GD k and transmitter n, and Φ is the duration of each time slot.

C. Channel Modeling

We consider a time-varying channel that changes from one time slot to another. In downlink systems, we assume that Doppler shift caused by the high-speed of LEO satellites

can be effectively pre(post)-compensated in the gateway with known GDs' position, satellites' orbits and satellites' speed [12]. At time slot t, a generic channel state between receiver k and transmitter n can be modeled as:

$$h_{k,n,t} = G_T \cdot G_C \cdot G_R, \tag{5}$$

where G_T and G_R are the antenna transmitting and receiving gain, respectively, and G_C represents the channel loss. For air-to-ground channel (from LEOs to GDs), G_C consider a Rician fading channel [8], which can be expressed as:

$$G_C = \left(\frac{c}{4\pi d f_c}\right)^2 \cdot G_H \cdot A(d) \cdot \varphi, \tag{6}$$

where c is the speed of light, d is the propagation distance between LEO and the terminals, f_c is the carrier frequency, G_H is the pitch angle fading, and φ is the Rician fading factor. $A(d)$ is the atmospheric loss which is expressed as:

$$A(d) = 10^{\left(\frac{3\chi d}{10h}\right)}, \tag{7}$$

where χ, in dB/km, is the attenuation through the clouds and rain, and h is the altitude of LEO. For terrestrial channel (from HD-TSTs and BSs to GUs), G_C consists of the path loss and Rayleigh small-scale fading [13], which is given by:

$$G_C = \left(\frac{c}{4\pi d f_c}\right)^2 \cdot \phi, \tag{8}$$

where ϕ is the Rayleigh fading factor.

III. Problem Formulation

In this section, we formulate an optimization problem for link group-time slot scheduling in LEO-terrestrial systems. We define binary variables $\mathbf{x} = [x_{1,1}, ..., x_{g,t}, ..., x_{G,T}]$ to indicate the scheduled groups, where

$$x_{g,t} = \begin{cases} 1, & \text{if group } g \text{ is scheduled at time slot } t, \\ 0, & \text{otherwise.} \end{cases}$$

In the objective design, considering the over-loaded scenario with densely deployed users, the system with limited resources may not be able to satisfy every user's data demand D_k. We then consider a composite utility function in (9), and define that GD k is served, i.e., $f_k(\mathbf{x}) = 1$, when a threshold $D'_k (D'_k < D_k)$ is satisfied.

$$f_k(\mathbf{x}) = \mathbb{1}\left(\sum_{t\in\mathcal{T}}\sum_{g\in\mathcal{G}} R_{k,g,t}x_{g,t} - D'_k\right), \tag{9}$$

where $\mathbb{1}(\cdot)$ is an indicator function such that

$$\mathbb{1}(a) = \begin{cases} 1, & \text{if } a > 0 \\ 0, & \text{if } a \le 0 \end{cases}. \tag{10}$$

We convert the non-linear function $f_k(\mathbf{x})$ to be linear function by introducing auxiliary variables $\mathbf{y} = \{y_1, ..., y_k, ..., y_K\}$ and linear constrains (11d), where $y_k = f_k(\mathbf{x})$. The optimization problem is formulated as:

$$\mathbf{P1}: \min_{x_{g,t}, y_k} \quad f(\mathbf{x}, \mathbf{y}) = \eta_0 \left(\sum_{k\in\mathcal{K}} y_k - K\right)^2 +$$

$$\sum_{k\in\mathcal{K}} \eta_k \left(\sum_{t\in\mathcal{T}}\sum_{g\in\mathcal{G}} R_{k,g,t}x_{g,t} - D_k\right)^2 \tag{11a}$$

$$s.t.\ \bar{\gamma}_k - \gamma_{k,g,t} \le V\left(1 - x_{g,t}\sum_{n\in\mathcal{N}}\alpha_{k,n,g}\right),$$

$$\forall k \in \mathcal{K}, g \in \mathcal{G}, t \in \mathcal{T}, \tag{11b}$$

$$\sum_{g\in\mathcal{G}} x_{g,t} \le 1,\ \forall t \in \mathcal{T}, \tag{11c}$$

$$D'_k y_k \le \sum_{t\in\mathcal{T}}\sum_{g\in\mathcal{G}} R_{k,g,t}x_{g,t},\ \forall k \in \mathcal{K}, \tag{11d}$$

$$x_{g,t} \in \{0,1\},\ \forall g \in \mathcal{G},\ t \in \mathcal{T}, \tag{11e}$$

$$y_k \in \{0,1\},\ \forall\ k \in \mathcal{K}, \tag{11f}$$

where $\bar{\gamma}_k$ is the SINR threshold of GD k, V is a positive sufficiently large value, and $\eta_0, ..., \eta_K$ are the weights controlling the impact of each gap. The objective (11a) aims at serving as many GDs as possible and delivering more data to GDs such that the two gaps in the overloaded system can be minimized. The first term in the objective is used to keep user fairness. The optimal scheduler is encouraged to meet the minimum requirement D'_k to serve more users and gain utility from the first term in the objective. Stimulating by the second term, when some users' weights η_k are considerable, consuming some resources and satisfying higher demand D_k can be a preferred option. The constraints are explained as follows:

- The constraints (11b) mean that if GD k is scheduled at time slot t, i.e., $x_{g,t}\sum_{n\in\mathcal{N}}\alpha_{k,n,g} = 1$, the SINR of GD k should be higher than the threshold $\bar{\gamma}_k$ to guarantee the quality of the links.
- The constraints (11c) represent no more than one group can be scheduled to a time slot based on the one-to-one transmission mode.
- The constraints (11d) mean that if GD k is successfully served, i.e., $y_k = 1$, the received data should be larger than the minimum requirement D'_k, which is consistent with Eq. (9).
- The constraints (11e)-(11f) are binary constraints for variables.

$\mathbf{P1}$ is a quadratic integer programming (QIP) problem. The relaxed problem of $\mathbf{P1}$ is convex since the symmetric matrix is positive semi-definite, such that $\mathbf{P1}$ can be solved optimally by branch and bound (B&B) [14]. However, the difficulty of $\mathbf{P1}$ lies at the combinatorial nature, leading to the exponential growth of the number of variables and the computational time.

IV. Solution Development

A. ADMM-Based Near-Optimal Algorithm

Being aware of the high complexity of the optimal solution, we develop an ADMM-HEU algorithm that first solves the relaxed problem of $\mathbf{P1}$ in a distributed way, then follows a centralized rounding operation to obtain integer solutions. Specifically, we relax $\mathbf{P1}$ to a quadratic programming (QP) problem, which is convex, by setting the integer variables $\mathbf{x}, \mathbf{y}$ to continuous variables $\hat{\mathbf{x}}, \hat{\mathbf{y}}$. The solutions of the QP

Algorithm 1 ADMM-HEU Algorithm

Inputs:

Parameters: D_k, D'_k and $R_{k,n,t}$.

Outputs:

Heuristic solution: $x^*_{g,t}$ and y^*_k

1: Initialize $\hat{\mathbf{x}}^0_t$, $\hat{\mathbf{y}}^0$, $\mathbf{z}^0$, $\boldsymbol{\lambda}^0$ and $i = 0$.
2: **for** $i = 0, .., I_{max}$ **do**
3: $\quad \hat{\mathbf{x}}^{i+1}_t = \underset{\hat{\mathbf{x}}_t \in \mathcal{X}_t}{\operatorname{argmin}} L(\hat{\mathbf{x}}^i_1, ..., \hat{\mathbf{x}}^i_T, \hat{\mathbf{y}}^i, \mathbf{z}^i, \boldsymbol{\lambda}^i),\ \forall t \in \mathcal{T}.$
4: $\quad \hat{\mathbf{y}}^{i+1} = \underset{\hat{\mathbf{y}} \in \mathcal{Y}}{\operatorname{argmin}} L(\hat{\mathbf{x}}^i_1, ..., \hat{\mathbf{x}}^i_T, \hat{\mathbf{y}}^i, \mathbf{z}^i, \boldsymbol{\lambda}^i).$
5: $\quad \mathbf{z}^{i+1} = \underset{\mathbf{z} \in \mathcal{Z}}{\operatorname{argmin}} L(\hat{\mathbf{x}}^i_1, ..., \hat{\mathbf{x}}^i_T, \hat{\mathbf{y}}^i, \mathbf{z}^i, \boldsymbol{\lambda}^i).$
6: $\quad \lambda^{i+1}_k = \lambda^i_k + \rho \left(z^i_k - D'_k \hat{y}^i_k + \sum_{g \in \mathcal{G}} \sum_{t \in \mathcal{T}} R_{k,g,t} \hat{x}^i_{g,t} \right).$
7: **end for**
8: Obtain relaxed solution $\hat{x}^*_{g,t}$.
9: **for** $t \in \mathcal{T}$ **do**
10: $\quad$ Find $g^\dagger = \underset{g \in \mathcal{G}}{\operatorname{argmax}} \{\hat{x}^*_{1,t}, ..., \hat{x}^*_{G,t}\}$.
11: $\quad$ Set $x^*_{g^\dagger,t} = 1$ and $x^*_{g,t} = 0, \forall g \neq g^\dagger$
12: **end for**
13: Calculate y^*_k based on (9).

problem provide a lower bound for $\mathbf{P1}$. However, the computational time of the conventional numerical optimization methods on solving QP, e.g., interior point method and semi-definite relaxation, could still be high due to the exponentially increasing number of variables. We notice that the objective function is separable, which motivates the development of the ADMM-based algorithm since it possesses the parallel computing capability and good convergence [15]. To apply ADMM, we decompose the relaxed variables into $T+1$ blocks $\hat{\mathbf{x}}_1, ..., \hat{\mathbf{x}}_T, \hat{\mathbf{y}}$, where $\hat{\mathbf{x}}_t = \hat{\mathbf{x}}_t = \{\hat{x}_{1,t}, ..., \hat{x}_{G,t}\}$, and introduce auxiliary variables $\mathbf{z} = \{z_1, ..., z_K\}$, where

$$z_k = D'_k \hat{y}_k - \sum_{g \in \mathcal{G}} \sum_{t \in \mathcal{T}} R_{k,g,t} \hat{x}_{g,t}, \forall k \in \mathcal{K}. \tag{12}$$

The inequality constraints (11d) are replaced by:

$$z_k \leq 0,\ \ \forall k \in \mathcal{K}. \tag{13}$$

The augmented Lagrangian function of the relaxed $\mathbf{P1}$ is expressed as:

$$\begin{aligned} &L(\hat{\mathbf{x}}_1, ..., \hat{\mathbf{x}}_T, \hat{\mathbf{y}}, \mathbf{z}, \boldsymbol{\lambda}) \\ =&f(\hat{\mathbf{x}}, \hat{\mathbf{y}}) + \sum_{k \in \mathcal{K}} \lambda_k \left(z_k - D'_k \hat{y}_k + \sum_{g \in \mathcal{G}} \sum_{t \in \mathcal{T}} R_{k,g,t} \hat{x}_{g,t} \right) \\ +&\frac{\rho}{2} \sum_{k \in \mathcal{K}} \| z_k - D'_k \hat{y}_k + \sum_{g \in \mathcal{G}} \sum_{t \in \mathcal{T}} R_{k,g,t} \hat{x}_{g,t} \|^2, \end{aligned} \tag{14}$$

where $\rho > 0$ is the penalty parameter and $\boldsymbol{\lambda} = \{\lambda_1, ..., \lambda_K\}$ are the lagrangian multipliers. ADMM minimizes (14) with respect to $\hat{\mathbf{x}}_1, ..., \hat{\mathbf{x}}_T, \hat{\mathbf{y}}, \mathbf{z}$ in an alternating direction manner, and updates λ_k accordingly. Starting from any initialization points, in each iteration i, ADMM update each block by the following rule until reaching the maximum iteration I_{max}:

$$\hat{\mathbf{x}}^{i+1}_t = \underset{\hat{\mathbf{x}}_t \in \mathcal{X}_t}{\operatorname{argmin}} L(\hat{\mathbf{x}}^i_1, ..., \hat{\mathbf{x}}^i_T, \hat{\mathbf{y}}^i, \mathbf{z}^i, \boldsymbol{\lambda}^i),\ \forall t \in \mathcal{T}, \tag{15}$$

$$\hat{\mathbf{y}}^{i+1} = \underset{\hat{\mathbf{y}} \in \mathcal{Y}}{\operatorname{argmin}} L(\hat{\mathbf{x}}^i_1, ..., \hat{\mathbf{x}}^i_T, \hat{\mathbf{y}}^i, \mathbf{z}^i, \boldsymbol{\lambda}^i), \tag{16}$$

$$\mathbf{z}^{i+1} = \underset{\mathbf{z} \in \mathcal{Z}}{\operatorname{argmin}} L(\hat{\mathbf{x}}^i_1, ..., \hat{\mathbf{x}}^i_T, \hat{\mathbf{y}}^i, \mathbf{z}^i, \boldsymbol{\lambda}^i), \tag{17}$$

where $\mathcal{X}_t = \{\mathbf{x}_t | (11b), (11c), (11d)\}$, $\mathcal{Y} = \{\mathbf{y} | 0 \leq y_k \leq 1\}$ and $\mathcal{Z} = \{\mathbf{z} | z_k \leq 0\}$.

We conclude ADMM-HEU in Alg. 1. In lines 1-8, ADMM is adopted to solve the relaxed problem of $\mathbf{P1}$. All the block variables and lagrangian multiplier are updated iteratively in the loop (in lines 2-7). Then, we collect the continuous solutions $\hat{x}^*_{g,t}$ (in lines 9-12). At time slot t, we perform binarization by setting the group with the largest $\hat{x}^*_{g,t}$ to 1 and the others to 0. In line 13, the sub-optimal y^*_k can be calculated by (9). In ADMM, the scales of the sub-problems in (15)-(17) are reduced and these tasks can be processed in parallel with a multi-core processor, thus improving computation efficiency.

Algorithm 2 LC-HEU Algorithm

Inputs:

D_k, D'_k and $R_{k,n,t}$.

Outputs:

Heuristic solution: $x^*_{g,t}$ and y^*_k.

1: Calculate ρ_k by (18).
2: **for** $t \in \mathcal{T}$ **do**
3: $\quad$ Observe currently received data $\hat{D}_{k,t}$.
4: $\quad$ Calculate $\rho'_{k,t}$ by (19).
5: $\quad$ Select N GDs with the largest gaps $\rho_k - \rho'_{k,t}$.
6: $\quad$ Filter the groups containing the selected GDs.
7: $\quad$ Determine the scheduled group $g^\dagger$ by (20).
8: $\quad$ Set $x^*_{g^\dagger,t} = 1$ and $x^*_{g,t} = 0, \forall g \neq g^\dagger$
9: **end for**
10: Calculate $\hat{y}^*_k$ based on (9).

B. Efficient Suboptimal Algorithm

The performance of ADMM-HEU depends on its convergence speed, and a large number of iterations may be required in large-scale scenarios. To further reduce the solving time, we propose an LC-HEU algorithm, as summarized in Alg. 2. From our observation, in the optimal strategy, the amount of data successfully received by GD k is positively associated with the average channel state $\bar{R}_k$, demands D_k and weights η_k, where $\bar{R}_k = \frac{\sum_{g \in \mathcal{G}} \sum_{t \in \mathcal{T}} R_{k,g,t}}{G \times T}$. We intuitively estimate that the ratio of the received data for GD k to the total received data is:

$$\rho_k = \frac{\eta_k D_k \bar{R}_k}{\sum_{k \in \mathcal{K}} \eta_k D_k \bar{R}_k},\ \forall k \in \mathcal{K}. \tag{18}$$

With ρ_k, we design a greedy method (in lines 2-9) for link group-time slot scheduling such that the actual ratio of the received data can approach the estimated one. Specifically, at time slot t, we first observe the currently received data $\hat{D}_{k,t}$

and calculated the current ratio $\rho'_{k,t}$ by:

$$\rho'_{k,t} = \frac{\hat{D}_{k,t}}{\sum_{k\in\mathcal{K}} \hat{D}_{k,t}}, \ \forall k \in \mathcal{K}. \tag{19}$$

Then, we select N GDs with the largest gaps $\rho_k - \rho'_{k,t}$, denoted by $\mathcal{K}^* = \{k_1, ..., k_N\}$, and filter a subset $\mathcal{G}^*$ from $\mathcal{G}$, where all the groups in $\mathcal{G}^*$ contains $\mathcal{K}^*$. The scheduled group at time slot t can be determined by:

$$g^\dagger = \underset{g\in\mathcal{G}^*}{\operatorname{argmax}} \sum_{k\in\mathcal{K}^*} R_{k,g,t}. \tag{20}$$

LC-HEU can dramatically reduce the computational time compared to the optimal algorithm since it avoids solving time-consuming optimization problems but the errors on estimation and approximation may bring gaps to the optimum.

V. Numerical Results

In this section, we evaluate the performance of the proposed heuristic schemes via numerical results. In the simulation, the parameter settings are similar as in [6]. The number of GDs varies up to 90 and the number of transmitters is 4, including 2 LEO, 1 BS and 2 TST. The altitude of LEO is 780 km. The service area is covered by a LEO beam with an area of 2800 (Km^2) [17]. The coverage area of BS and TST are 28 (Km^2) and 0.125 (Km^2), respectively. We assume the time limitation for transmission T is set from 5 to 15 time slots. The duration of time slot Φ is set to 0.1 (s). The transmit power of LEO, BS and TST are set to 100 (Watt), 40 (Watt) and 2 (Watt), respectively [16]. The bandwidth for C-band communications is 20 (MHz) and for Ka-band communications is 400 (MHz). The carrier frequency of Ka-Band and C-band are 30 (GHz) and 4 (GHz), respectively. The noise power spectral density is -174 (dBm/Hz).

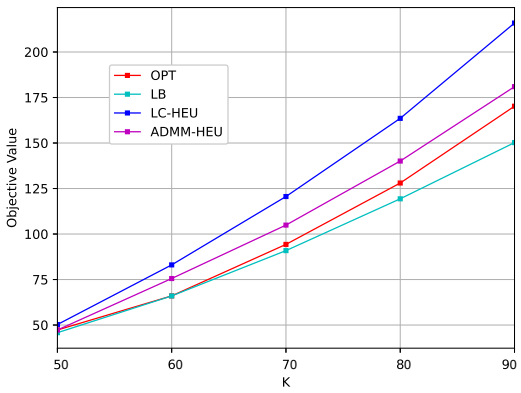

Figure 2. Objective value vs. number of GDs

We compare the proposed heuristic algorithms in terms of the objective value and computational time with the optimal algorithm (OPT), and we provide the lower bound (LB) which is obtained by solving the relaxed problem of **P1**. Fig. 2 shows the objective value with the number of GDs. We can observe that the objective value increases with K since, with limited power and spectrum, a larger K means less received data per user. ADMM-HEU has 6.67% gap to the optimum on average, while for LC-HEU, the gap is 20.08%. In addition, the results of LB and OPT almost overlap when $K \leq 60$, but when K continues to increase, the gap between OPT and LB widens.

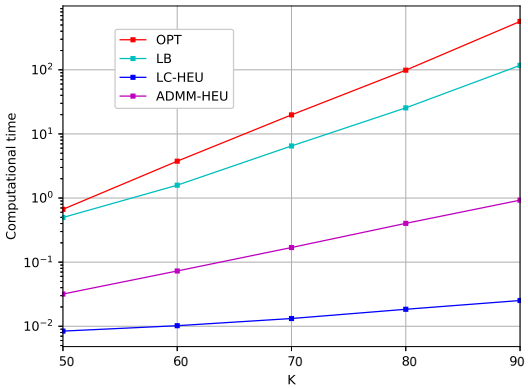

Figure 3. Computational time vs. number of GDs

Fig. 3 demonstrates the objective value with respect to T. For all the algorithms, the objective value reduces by around 66% from $T = 5$ to $T = 15$. This is because, under the fixed transmission power, a smaller T means a shorter time for data delivery and less transmitted data, leading to an increase of the supply-demand gap. When the transmission time T is sufficient, e.g., $T > 14$, ADMM-HEU and LC-HEU approach to OPT, with the gap of 3.47% and 8.86% respectively.

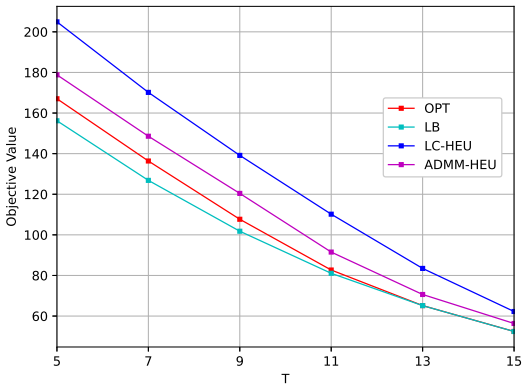

Figure 4. Objective value vs. number of time slots

Fig. 4 compares the computational time between the solutions. OPT consumes the most computational time, reaching 5000s when $K = 90$. The reason for the inefficiency lies in that the complexity of B&B method exponentially increases with the number of variables, which also exponentially increases with K. The computational time of obtaining LB is 67.67% lower than OPT since solving the relaxed QP problem is more time-saving than the original QIP problem. Compared to OPT, ADMM-HEU saves 98.14% computational time by decomposing variables into multiple blocks and performing

distributed calculations, and for LC-HEU, the computational time reduces by 99.93% as it avoids solving optimization problems. In addition, LC-HEU keeps the computational time at millisecond-level even if the number of GDs grows to 90. However, by recalling Fig. 2, LC-HEU sacrifices 15.43% performance gain in objective value compared with ADMM-HEU.

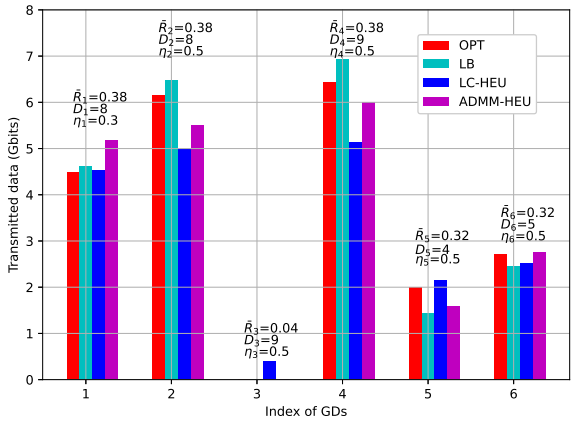

Figure 5. Transmitted data vs. the index of GDs

Fig. 5 shows the distribution of transmitted data over the GDs, where the x-axis is the index of GDs and the y-axis is the volume of transmitted data. We simulate a 6-user case and record the performance values within $T = 10$ time slots. From the results, the GDs with a larger weight can have a higher priority to be scheduled, e.g., GD 2 with $\eta_2 = 0.5$ receives more data than GD 1 with $\eta_1 = 0.3$. The GDs with poor channel state receive less data, e.g., the transmitted data for GD 3, with $\bar{R}_3 = 0.04$, is close to 0. Moreover, by comparing GD 5 with $D_5 = 4$ and GD 6 with $D_6 = 5$, the GDs with more data requests are inclined to be transmitted more data. The mean square error on all GDs between OPT and ADMM-HEU is 0.19 while for LC-HEU, due to the inaccuracy of the estimated ratio ρ_k, the mean square error is 1.22.

VI. Conclusion

We have investigated a resource scheduling problem in LEO-assisted communication systems to minimize the gap between the transmitted data and GDs' demands, and the gap between the number of successfully served GDs and total GDs. Due to the combinatorial nature of the optimization, the optimal approach, i.e., B&B, has exponential increasing computational time. Toward efficient solutions, we propose two heuristic algorithms, where ADMM-HEU improves efficiency by distributed calculation while LC-HEU saves computational time by avoiding addressing optimization problems. Numerical results show the effectiveness of the proposed algorithms on improving computation efficiency.

Acknowledgment

The work has been supported by the FNR CORE projects ROSETTA (C17/IS/11632107) and ASWELL (C19/IS/13718904), and by the FNR bilateral project LARGOS (12173206).

References

[1] L. Lei, Y. Yuan, T. X. Vu, S. Chatzinotas, M. Minardi and J. F. M. Montoya, "Dynamic-adaptive AI solutions for network slicing management in satellite-integrated B5G systems," in *IEEE Network*, vol. 35, no. 6, pp. 91-97, Dec. 2021.

[2] 3GPP TR 23.737, "Study on architecture aspects for using satellite access in 5G (release 17)".

[3] J. Wu, C. Yuen, N. M. Cheung, and J. Chen, "Delay-constrained high definition video transmission in heterogeneous wireless networks with multi-homed terminals," in *IEEE Transaction on Mobile Computing*, vol. 15, no. 3, pp. 641–655, Mar. 2016.

[4] O. Kodheli et al., "Satellite communications in the new space era: a Survey and future challenges," in *IEEE Communications Surveys and Tutorials*, vol. 23, no. 1, pp. 70-109, 2021.

[5] L. You, K. Li, J. Wang, X. Gao, X. Xia, and B. Ottersten, "Massive MIMO transmission for LEO satellite communications," in *IEEE Journal on Selected Areas in Communications*, vol. 38, no. 8, pp.1851-1865, Jun. 2020.

[6] B. Di, H. Zhang, L. Song, Y. Li, and G. Y. Li, "Ultra-dense LEO: integrating terrestrial-satellite networks into 5G and beyond for offloading," in *IEEE Transactions on Wireless Communications*, vol. 18, no. 1, pp. 47-62, Dec. 2018.

[7] Y. Li, N. Deng, and W. Zhou, "A hierarchical approach to resource allocation in extensible multi-layer LEO-MSS," in *IEEE Access*, vol. 8, pp.18522-18537, Jan. 2020.

[8] S. Wang, Y. Li, Q. Wang, M. Su, and W. Zhou, "Dynamic downlink resource allocation based on imperfect estimation in LEO-HAP cognitive system," in Proc. *2019 IEEE International Conference on Wireless Communications and Signal Processing (WCSP)*, Oct. 2019.

[9] F. Tian, L. Huang, G. Liang, X. Jiang, S. Sun, and J. Ma, "An efficient resource allocation mechanism for beam-hopping based LEO satellite communication system," in Proc. *2019 IEEE International Symposium on Broadband Multimedia Systems and Broadcasting (BMSB)*, Jun. 2019.

[10] A. Wang, L. Lei, E. Lagunas, S. Chatzinotas, A. I. P. Neira, and B. Ottersten, "Joint beam-hopping scheduling and power allocation in NOMA-assisted satellite systems," in Proc. *2021 IEEE Wireless Communications and Networking Conference (WCNC)*, Apr. 2021.

[11] W. Wang, Y. Tong, L. Li, A. A. Lu L. You, and X. Gao, "Near optimal timing and frequency offset estimation for 5G integrated LEO satellite communication system," in *IEEE Access*, vol. 7, pp. 113298-11331, 2019.

[12] "Doppler compensation, uplink timing advance and random access in NTN," 3GPP TSG RAN WG1 Meeting, no. 97, R1-1906087, May 2019.

[13] Y. Ruan, Y. Li, R. Zhang, W. Cheng, and C. Liu, "Cooperative resource management for cognitive satellite-aerial-terrestrial integrated networks towards IoT," in *IEEE Access*, vol. 8, pp. 35759-35769, 2020.

[14] C. H. Papadimitriou and K. Steiglitz, "Combinatorial optimization: algorithms and complexity," Mineola, NY, USA: Dover, 1998.

[15] S. Boyd, N. Parikh, and E. Chu, "Distributed optimization and statistical learning via the alternating direction method of multipliers," Hanover, MA, USA: Now Publishers Inc., 2011.

[16] O. Popescu, "Power budgets for cubesat radios to support ground communications and inter-satellite links," in *IEEE Access*, vol. 5, pp. 12618-12625, 2017.

[17] S. Xia, Q. Jiang, C. Zou and G. Li, "Beam coverage comparison of LEO satellite systems based on user diversification," in *IEEE Access*, vol. 7, pp. 181656-181667, 2019.